Article

Satellite-Based Analysis of Spatiotemporal Wildfire Pattern in the Mongolian Plateau

Yulong Bao [1,†], Masato Shinoda [2], Kunpeng Yi [3,*,†], Xiaoman Fu [1], Long Sun [4], Elbegjargal Nasanbat [5], Na Li [6], Honglin Xiang [4], Yan Yang [4], Bulgan DavdaiJavzmaa [7] and Banzragch Nandintsetseg [8]

1   College of Geography Science, Inner Mongolia Normal University, Hohhot 101022, China
2   Graduate School of Environmental Studies, Nagoya University, Nagoya 4648601, Japan
3   State Key Laboratory of Urban and Regional Ecology, Research Center for Eco-Environmental Sciences, Chinese Academy of Sciences, Beijing 100085, China
4   Key Laboratory of Sustainable Forest Ecosystem Management-Ministry of Education, School of Forestry, Northeast Forestry University, Harbin 150040, China
5   SILVIS Lab, Department of Forest and Wildlife Ecology, University of Wisconsin-Madison, 1630 Linden Drive, Madison, WI 53706, USA
6   School of Economics Management, Inner Mongolia Normal University, Hohhot 101022, China
7   National Remote Sensing Center of Mongolia, Juulchiny street-5, Ulaanbaatar 15160, Mongolia
8   Eurasia Institute of Earth Sciences, Istanbul Technical University, Istanbul 34469, Turkey
*   Correspondence: kpyi@rcees.ac.cn
†   These authors contributed equally to this work.

Abstract: Burned area is a critical input to biomass burning carbon emissions algorithms and for understanding variability in fire activity due to climate change. This study presents the spatial and temporal patterns of wildland fires in the Mongolian Plateau (MP) using Collection 6 NASA MCD64A1 500 m global Burned Area product from 2001 to 2021. Both inter- and intra-annual fire trends and variations in two subregions, Mongolia and China's Inner Mongolia, were analyzed. The results indicated that an average area of 1.3×10^4 km^2 was consumed by fire per year in the MP. The fire season has two peaks: spring (March, April, and May) and autumn (September, October, and December). The profiles of the burnt area for each subregion exhibit distinct seasonality. The majority of wildfires occurred in the northeastern and southwestern regions of the MP, on the border between Mongolia and China. There were 2.7×10^4 km^2 of land burned by wildfires in the MP from 2001 to 2021, 57% of which occurred in spring. Dornod aimag (province) of Mongolia is the most fire-prone region, accounting for 51% of the total burned area in the MP, followed by Hulunbuir, at 17%, Sukhbaatar, at 9%, and Khentii at 8%. The changing patterns of spatiotemporal patterns of fire in the MP were analyzed by using a spatiotemporal cube analysis tool, ArcGIS Pro 3.0.2. The results suggested that fires showed a decreasing trend overall in the MP from 2001 to 2021. Fires in the southern region of Dornod aimag and eastern parts of Great Xing'an Mountain showed a sporadic increasing trend. Therefore, these areas should be priorities for future fire protection for both Mongolia and China.

Keywords: wildfire; burned area; MODIS; Mongolian Plateau; climate change

1. Introduction

Global warming is often implicated as the primary driver of accelerated wildfire activity and drought events [1,2]. A vivid manifestation is the several large wildfires that have occurred on an unprecedented scale and duration recently [3,4], such as wildfires in Australia in 2019 to 2020 [5,6], the Amazon rainforest in Brazil in 2019 and 2020 [7], the western United States in 2018 and 2020 [8,9], and Canada from 2016 to 2018 [10,11]. The Intergovernmental Panel on Climate Change (IPCC) reports that Earth's average surface temperature is projected to hit 1.5 °C (2.7 °F) or 1.6 °C (2.9 °F) above pre-industrial levels around 2030 [12]. Two degrees of warming could destroy ecosystems on about 13%

of the world's land area, increasing the risk of extinction for many insects, plants, and animals. Mongolia offers a glimpse into the future, as it has already experienced significant climate changes, with a warming of over 2 °C and declines in rainfall reported between 1940 and 2015 [13]. The Mongolian Plateau (MP) is a typical pastoral region in the world, with animal husbandry as the main economic production mode. Hence, the MP's people depend highly on their natural ecosystem [14]. Herders' ancient lifestyle is facing a threat from climate change that is greater than ever before [15]. Unprecedented extreme episodes of hotter and drier climate from 2000 to 2020 in the MP are caused by a positive feedback loop between fuels' moisture deficits and land surface warming, and potentially represent the start of an irreversible trend [16]. Leaf area index (LAI) and fractional vegetation cover (FVC) presented a decreasing trend since 1982 in the MP, especially in Khentii and Dornod aimags(provinces) of Mongolia [17]. In addition, a decreasing trend of net primary productivity (NPP) was observed, which indicated that a total of 60.55–87.75% of land in Mongolia experienced drought [18]. As a result, more and more herders are dismantling their yurts and abandoning the vast steppe to settle in the cities. The MP faces rates of warming far higher than the global average due to its relatively homogenous steppe desert ecosystem and low annual precipitation. Warming in maximum and minimum daily temperatures is expected to be faster than the average rate, potentially amplifying the stress exerted on livestock, livelihoods, and ecosystems in the MP. Recent climate changes in the MP have led to chronic drought [15,19–21] and increased exposure to secondary impacts such as wildfires [22] and dust storms [23]. Recently, extreme climate-driven hazards have occurred in MP more frequently than ever before. Steppe ecosystems in the plateau are especially vulnerable to climate change due to arid and semi-arid climates and homogeneity. After these extreme disasters, livestock and wildlife species were weakened or killed because of food shortages.

Wildfire has been one of the typical disasters in the main region of the temperate steppe in the MP; wildfires have caused catastrophic damages due to their complex interaction with the steppe ecosystems and livelihoods [22,24,25]. Steppe fire is a limiting factor of livestock food resources, causing local ecological problems and posing large-scale implications for the economic and social crisis [26,27]. Understanding the distribution pattern of wildfires is essential to predicting whether and to what extent fires will occur in the future. The Moderate Resolution Imaging Spectroradiometer (MODIS) played an important role in fire monitoring. Satellite offers the advantages of extensive regional coverage and zero disturbances of the area to be viewed, and is a method for acquiring data in less accessible areas on a regular and cost-effective basis [28–30]. The MODIS Collection 6 MCD64A1 Burned Area product, which maps the spatial extent and approximate date of biomass burning worldwide at a spatial resolution of 500 m, has been used to carry out a broad range of research concerning on biomass burning over the past decades [31–34]. An accuracy assessment study indicated that MCD64 C6 detects more BA than C5.1, showing a better performance in small scars [34,35]. The Collection 6 MCD64A1 Burned Area product decreases the omission error in 90% of the analyzed area and increases the burn hits, providing improved BA estimates in 61% of the study area [35,36].

The recent record-breaking wildfire events, unprecedented losses, and escalating suppression costs in the MP have raised concerns about wildfire causes, patterns, and trends [37,38]. Focus is needed on the interplay between climate changes and current development trends in the MP. Unplanned development in fire-prone areas and air pollution issues could interact with climate changes to enhance health risks and inequalities. However, there has been little quantitative research on fires in the MP [22,24]. Our current understanding of large-scale steppe fire dynamics is insufficient to fully characterize their role in the grass-herd economic system. Hence, in this study, we specifically attempt to achieve the following three objectives: (1) to map and visualize the spatial and temporal distributions of fires in the MP; (2) to analyze the changing trend of wildfire patterns in the MP from 2001 to 2021; and (3) to quantitatively analyze the wildfire situation in the fire-prone areas.

2. Materials and Methods

2.1. Study Area

The MP (37°22′~53°20′N, 87°43′~126°04′E) is located in the hinterland of temperate Asia, covering a territory of 2.74 × 10^6 km^2, of which over 1.82 × 10^6 km^2 (66.29%) is natural steppe, including the Mongolia (57%) (MG) and the Inner Mongolia Autonomous Region (43%) (IM) in China. The MP sustains the eastern part of the Eurasian Steppe and represents the fifth-largest desert area on Earth, playing a crucial role in the global carbon cycle and climate system but also being prone to the risks of desertification. The plateau is an arid and semi-arid continental climate, with warm summers but long and cold winters when snowfall is common and persistent. The annual average temperature varies from −1.7 °C to 5.6 °C, with common temperature extremes due to the high elevation and deep continentality. Precipitation varies spatially, fluctuating, from year to year, from 90 to 433 mm, and mainly distributes between May and September. Vast steppe and desert steppe characterize the plateau, dotted with numerous lakes (Figure 1) nourishing the Mongolian people, creating a unique Mongolian nomadic civilization, and supporting a population of over 28 million by 2017.

2.2. Data Source and Processing

The primary purpose of this study was to identify patterns of burned areas in the MP. Satellite data is essential to obtain a clear and independent picture and understand long-term trends. The Collection 6 MCD64A1 Burned Area data used in this study were obtained from a span of 20 years, providing a more consistent spatial and temporal basis for interpretation than statistics compiled from different sources or short periods. The MCD64A1 product is defined for the global land surface from November 2000 to the present, in the equal-area sinusoidal projection of approximately 1200 × 1200 km tiles, which was distributed as a monthly product with each 500 m pixel classified as burned, unburned, or unmapped. The Collection 6 Burned Area product (MCD64A1), uses a refined algorithm designed to increase the detection of small burns, reduce the uncertainty in the timely detection of the day of burning, and reduce the extent of unmapped areas in regions with high cloud cover. We evaluated Mongolia and Inner Mongolia as two subregions of the MP. To analyze the fuel type, we used the "Esri 2020 Land Cover" dataset (resolution 10 m × 10 m) produced by Impact Observatory for Esri Inc. [39]. The Esri 2020 Land Cover map in the MP is shown in Figure 1. The Land Cover map uses Sentinel-2 satellite imagery with a 10 m resolution and a land classification model to classify the Earth's surface into 10 categories, namely, crops, water, trees, grass, flooded vegetation, built area, scrub/shrub, bare ground, snow/ice, and clouds for areas with no data.

In addition, the standardized precipitation index (SPI) and normalized difference vegetation index (NDVI) were used to show the temporal relationship with fire activities. The SPI was created for differing periods of 1 to 12 months by quantifying observed precipitation as a standardized departure from a selected probability distribution function that models the raw precipitation data. The raw precipitation data of MP were obtained from ERA5 dataset from 2001 to 2021 (https://www.ecmwf.int/en/forecasts/datasets/reanalysis-datasets/era5 (accessed on 23 December 2023)). A 16-day NDVI dataset from the MODIS C6 (MOD13A1) was used to extract the seasonality of vegetation phenology in the MP. Figure 2 shows the technical route of the study.
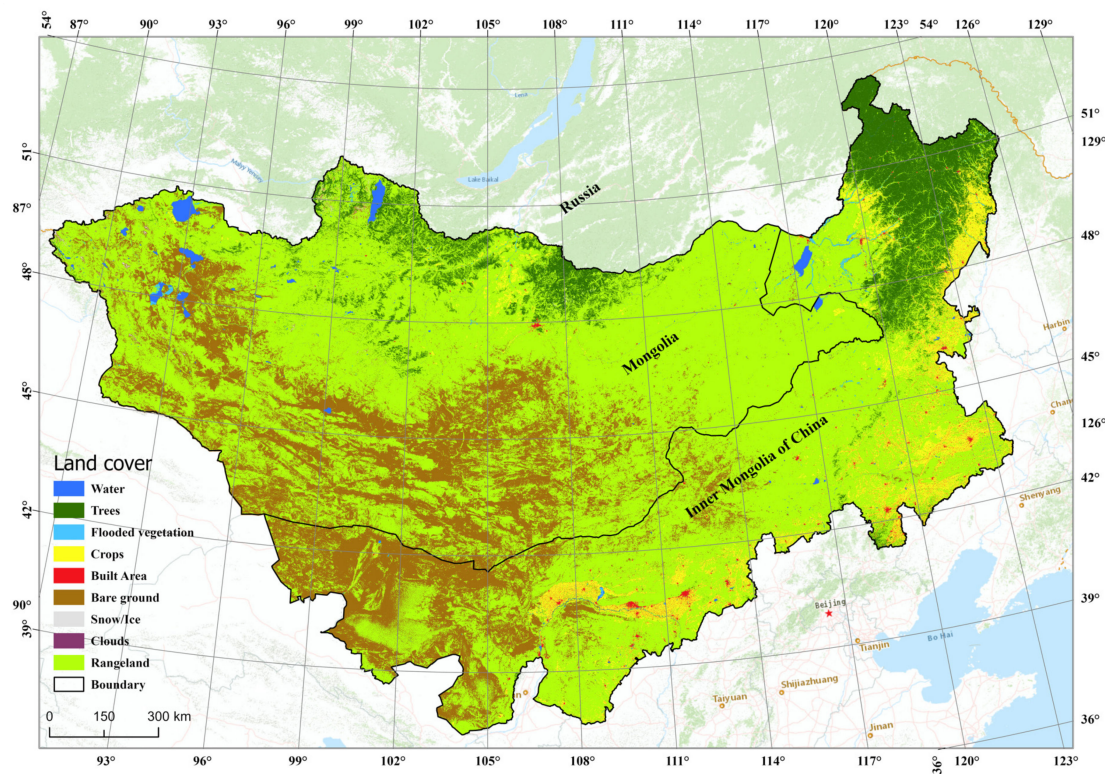
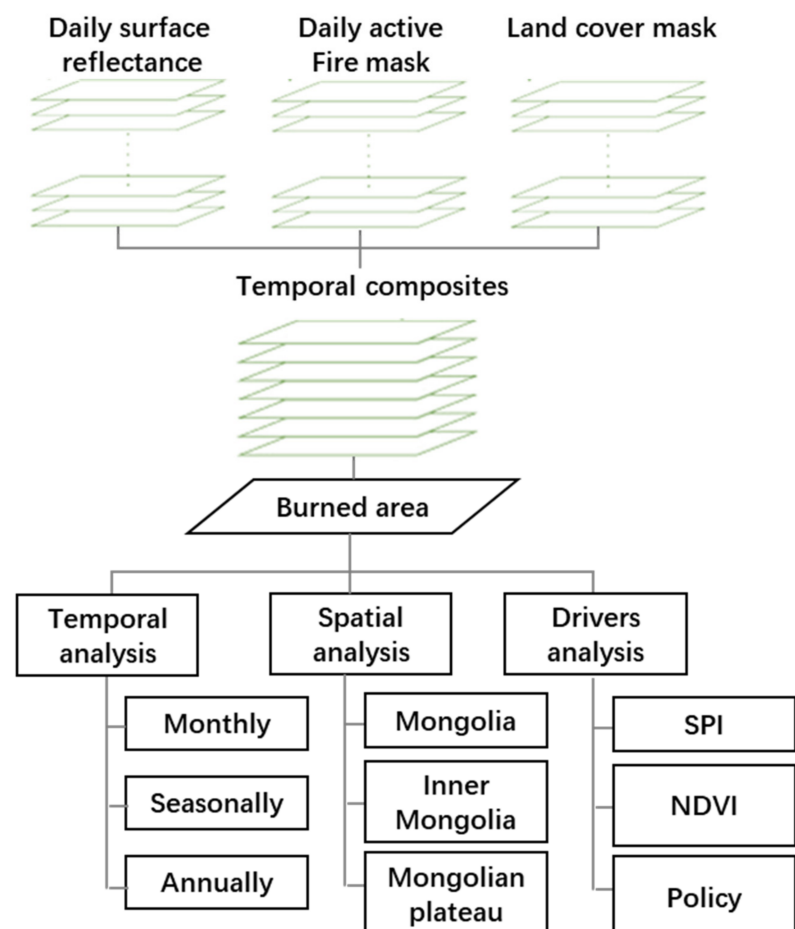**Figure 1.** Land cover pattern in the Mongolian Plateau (MP).

Figure 2. The technical route of the study.

2.3. Wildfire Pattern Analysis

The Space-Time Pattern Mining toolbox in ESRI ArcGIS Pro 3.0.2 software was used to analyze the spatial and temporal patterns of wildfire activity in the MP. Burned area information in pixels in the MP was transferred to points, which was used to aggregate into space–time bins by using the Create Space Time Cube tool. By counting the number of steppe fire points contained in each spatiotemporal cube, the steppe fire points are aggregated into the spatiotemporal bars of each spatial grid. All fire data points were aggregated into space–time bins to a 10 km hexagonal grid over the plateau, providing an overview of fire distribution that occurred on the plateau over the entire 20-year period from 2001 to 2021. Each bin is basically a cell in 3D. A location, or bin time series, represents a specific X, Y spatial extent through the entire time extent. Space–time cubes allow for the display and analysis of the data in three dimensions, with the fire locations represented on the *x*- and *y*-axes, and the years represented on the Z-axis. The dataset was used to produce space–time cubes to be able to explore the changes with trend data created from the Mann–Kendall trend test, which compares each bin value with that of the previous year. Positive values indicate inter-annual increases, negative values show decreases, and zero indicates no change. The space–time wildfires in annual, spring, and autumn patterns in MP were analyzed using the Getis Ord Gi* statistic of the emerging hotspot analysis tool (Supplementary Materials Table S1). Getis Ord Gi* statistic examined neighboring bins in both space and time. Hot spots account for an increasing trend in the consistency and intensity of the burned area of the yearly time step, while cold spots represent a decreasing trend.

3. Results

3.1. Temporal Pattern

3.1.1. Inter-Annual Trend

The MP has a vast area, spanning over 30 latitudes, and its internal geographical conditions and climate vary widely. We presented the first high-resolution fire history in the MP covering 2001 to 2021. The bars in Figure 3 show the burnt areas of vegetation, including forests and grassland. The MP has seen an average of 1.0×10^4 wildfires a year over the past 21 years, burning an average of 1.3×10^4 km^2 per year (see Figure 3a). The extent of area burned by wildfires each year appears to have a fluctuating downward trend. The annual burned area in the latter decade (2012–2021) declined by 38% compared to the previous decade (2001–2010). The peak burned area year occurred in 2003, with 2.7×10^4 km^2 of vegetated lands burned, which was twice the average annual burned area (1.3×10^4 km^2) from 2001 to 2021 and 13 times greater than a minor area burned in 2021 (0.2×10^4 km^2). Burned areas in the MP have declined by 91% from 2015 to 2021. The seasonal pattern of fire activities also varies considerably from year to year. However, the feature that spring and autumn are the primary fire seasons was confirmed in each year (Figure 3b). Although fires were almost absent in winter in the plateau, a few fires occurred in years of extreme drought with little snowfall, such as 2019 (Figure 3b). Summer is also not the primary burning season in the MP; however, a certain number of fires occurred, due to the low water content of the vegetation in drought years.

3.1.2. Intra-Annual Pattern

Fire is a natural phenomenon that impacts human behaviors, vegetation, and landscape functions. Fire was also an essential process in steppe-dominated ecosystems in the MP. As weather, vegetation, and human activities change with the seasons of the year, so do the incidence, causes, and severity of wildfires. Spring is the season with the high incidence of forest and steppe fires in the MP due to high biomass, windy and dry weather, and less rainfall. Spring fires fueled by dead grasses and shrubs from the previous winter tend to burn in the time between snowmelt and green-up. The MP has experienced devastating spring fires in recent years. According to our results, there were 2.7×10^4 km^2 of vegetated lands burned in the MP from 2001 to 2021. 57% of burned area occurred in

spring (Figures 3b and 4). These spring fires have coincided with extreme fire weather conditions during periods of strong winds coincident with unusually dry grasslands and forests enabled by anomalously warm conditions. Approximately 22% of the burned area was produced in summer, and 20% was produced in autumn. Fire incidence is at its lowest in the winter in the MP (Figure 4). In cold winter, fuel in the MP was covered by thick snow, and almost no wildfire occurred in winter; however, some crop residues burnings were detected by our study in the eastern region of Great Xing'an Mountain.
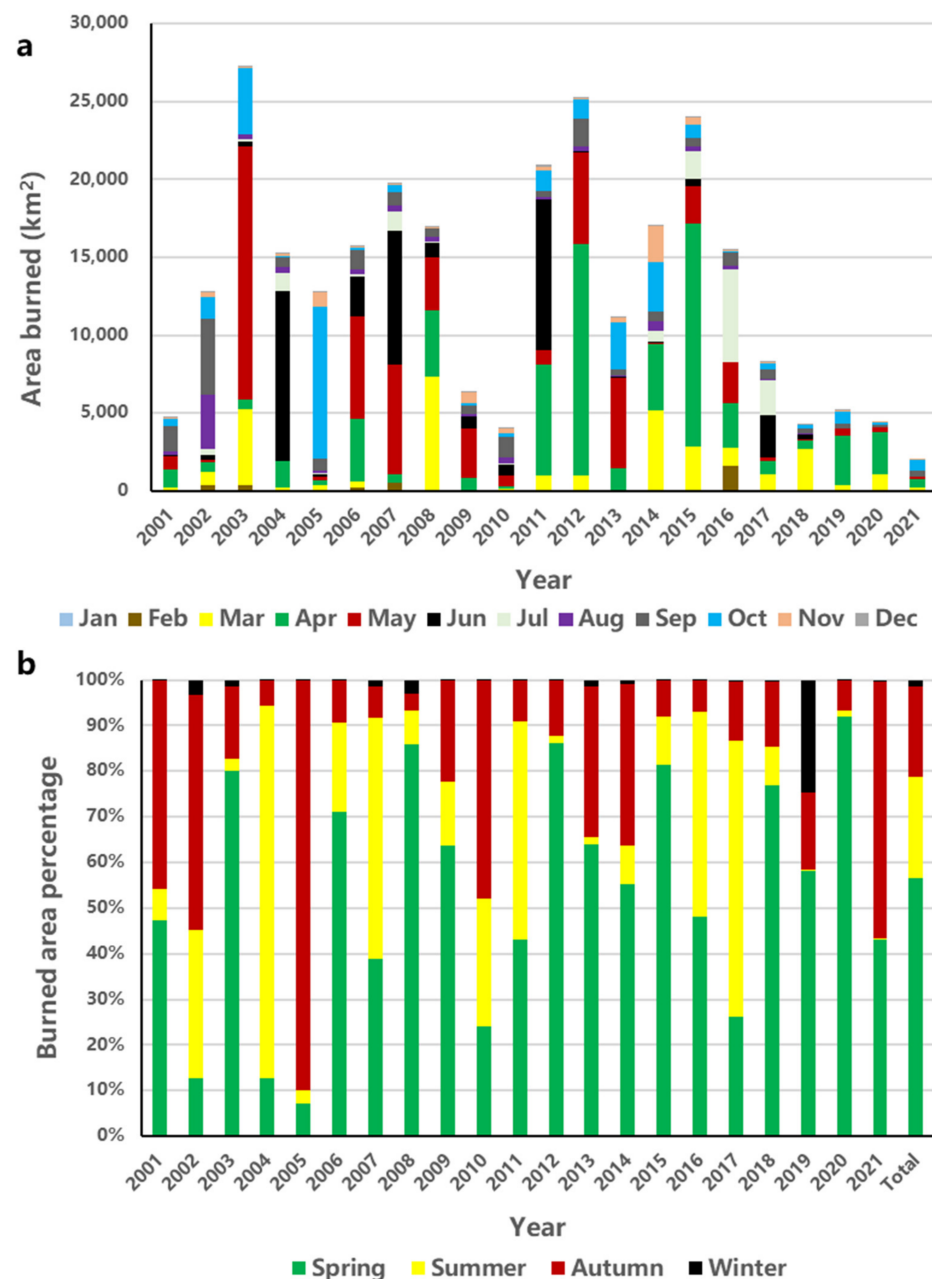

Figure 3. Annual (**a**) and seasonal (**b**) wildfire pattern in the Mongolian Plateau (MP) from 2001 to 2021.
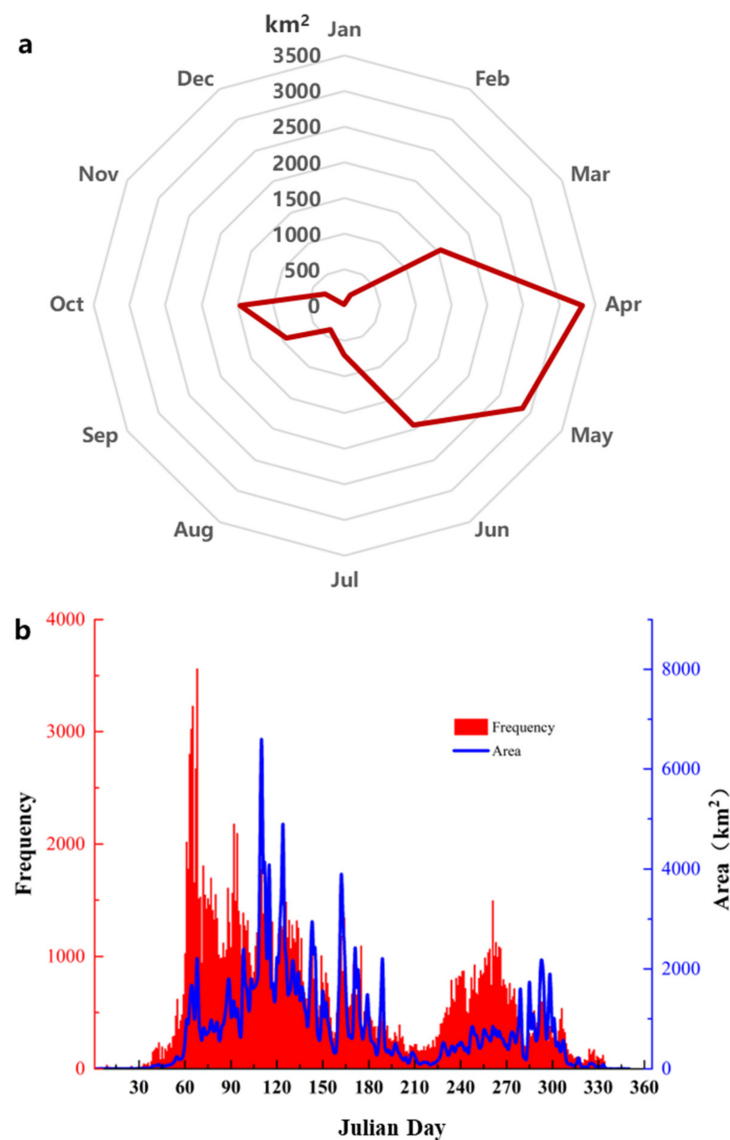
Figure 4. Fire temporal pattern in the Mongolian Plateau (MP) from 2001 to 2021. (**a**), monthly pattern; (**b**), daily pattern.

Fire season was defined as the time of year that wildfires are most likely to take place. In the MP, wildfires start in late March and early April, immediately after snow melts, when forest fuels are drying rapidly on southern- and western-facing slopes. The fire season was mainly from March through November, with two peaks. One peak is during spring (from March to May) and accounts for 57% of all burned areas (Figures 3b and 4a). The other fire peak falls within a short period in September to October. In summer, fires rarely occur, due to green-up and a relative increase in precipitation. However, in the mountain forest zone, especially in the high elevations, lightning storm activity is very common and increases considerably in June and July (Figures 3b and 4a). Specifically, wildfires in the MP mainly occurred on 88–192 Julian days (29 March to 11 July) and 249–299 Julian days (22 August to 26 October) during the year (Figure 4b).

3.2. Spatial Distribution

Spatial and seasonal variability in fire activity is apparent at the subregions and the MP scales (Figure 5). We show a merger of the spatially explicit 2001–2021 annual area burned in Figure 5. The spatial distribution of fires in the MP is highly uneven. It is important to note that fire-prone regions are mainly located in the eastern and northern parts of the

plateau, with 77% of the total burned area of the whole period occurring in Mongolia and only 23% of burned area in Inner Mongolia, China, from 2001 to 2021 (Figure 5). The China–Mongolia border is 4710 kilometers long. Frequent mega wildfires often cross the border in the MP, which has become an important ecological challenge shared by both countries and has given rise to several diplomatic issues. Our study indicated that not all regions near the border are threatened by wildfire. Only 1300 km, in the northeastern part of the entire 4710 km border length, is a high fire-risk region. Steppe fires mainly occurred in the spring season in the China–Mongolia border regions, which was also highlighted by the previous study [40]. We mapped and highlighted the burned area distribution in this region by buffering the 100 km zone along the border (Supplementary Materials Figure S2). The result highlighted that the most fire-prone region is only 10% of the land area of the MP, yet it is home to 90% of all burned areas. Most of the fires occur mainly followed by wind direction on the Mongolian side and spread from west to east, or south to north, towards the Chinese side, under the influence of the continental monsoon. It is worth noting that 90% of the fire incidents were successfully stopped at the borderline, with only a few megafires invading China's side (Supplementary Materials Figures S1 and S2). In this highlighted region, Mongolia hosts 97% of the area burned, with only 44% of the land, while less than 3% of the burned area was located on the Chinese side (Supplementary Materials Figure S2). Other critical fire-prone areas are the northern forest in Selenge and the steppe in Khentii, Dornod, and Sukhbaatar aimags, especially the regions near the Mongolia–Russia border. On the administrative level, Dornod Aimags of Mongolia is the most fire–prone region, accounting for 51% of the total burned area in the MP, followed by Hulunbuir, at 17%, Sukhbaatar, at 9%, Khentii, at 8%, Selenge, with 3%, and the other provinces/amigs together, accounting for less than 12% (Figure S1).

3.3. The Changing Trend of Wildfire Pattern

Using a spatiotemporal cube analysis tool, we have analyzed the changing patterns of spatiotemporal patterns of fire in the Mongolian plateau throughout the year and the two main fire seasons of spring and autumn. The results show that the MP fires show four trends (Figure 6). Firstly, oscillating cold spot (▨), which was defined as a statistically significant cold spot for the final time step interval, with a history of also being a statistically significant hot spot during a prior time step. Less than 90% of the time step intervals have been statistically significant cold spots. This trend accounts for 55.6% of annual fires, 59.8% of spring fires, and 57.7% of autumn fires (Supplementary Materials Figure S3 and Figure 6). The changing trend of wildfires in an oscillating decreasing trend mainly occurred in the northern forest in Selenge and the steppe in Khentii, Dornod, and Sukhbaatar aimags, especially the regions near the Mongolia–Russia and Mongolia–China borders. Fires in the southern parts of the Great Xing'an Mountain region also showed an oscillating decreasing trend. The second trend was sporadic cold spot (▨), which was defined as a statistically significant cold spot for the final time step interval, with a history of also being an on-again and off-again cold spot. Less than 90% of the time step intervals have been statistically significant cold spots, and none of the time step intervals have been statistically significant hot spots. This trend accounts for 6.2% of annual fires, 4.8% of spring fires, and 10.7% of autumn fires (Supplementary Materials Figure S3 and Figure 6). The changing trend of wildfires in a sporadic decreasing mode mainly occurred in southeastern parts of Inner Mongolia, China. The third trend was oscillating hot spot (▨), which was defined as a statistically significant hot spot for the final time step interval, which has a history of also being a statistically significant cold spot during a prior time step. Less than 90% of the time step intervals have been statistically significant hot spots. This trend accounts for 2.7% in annual fires, 5.7% in spring fires, and 6.2% in autumn fires (Supplementary Materials Figure S3 and Figure 6). The changing trend of wildfires in a sporadic increasing mode mainly occurred in a southern region of Dornod aimag in spring, and in eastern parts of the Great Xing'an Mountain in China in autumn. The final trend was persistent cold spot (■), which was defined as a location that has been a statistically significant cold spot for

90% of the time step intervals, with no discernible trend in the intensity of clustering of counts over time. This trend accounts for 9.7% of annual fires, 3.9% of spring fires, and 10.7% of autumn fires (Supplementary Materials Figure S3 and Figure 6). The changing trend of wildfires in a persistent decreasing mode mainly occurred in the Xilingol League of Inner Mongolia, China, and the northeastern part of Mongolia.
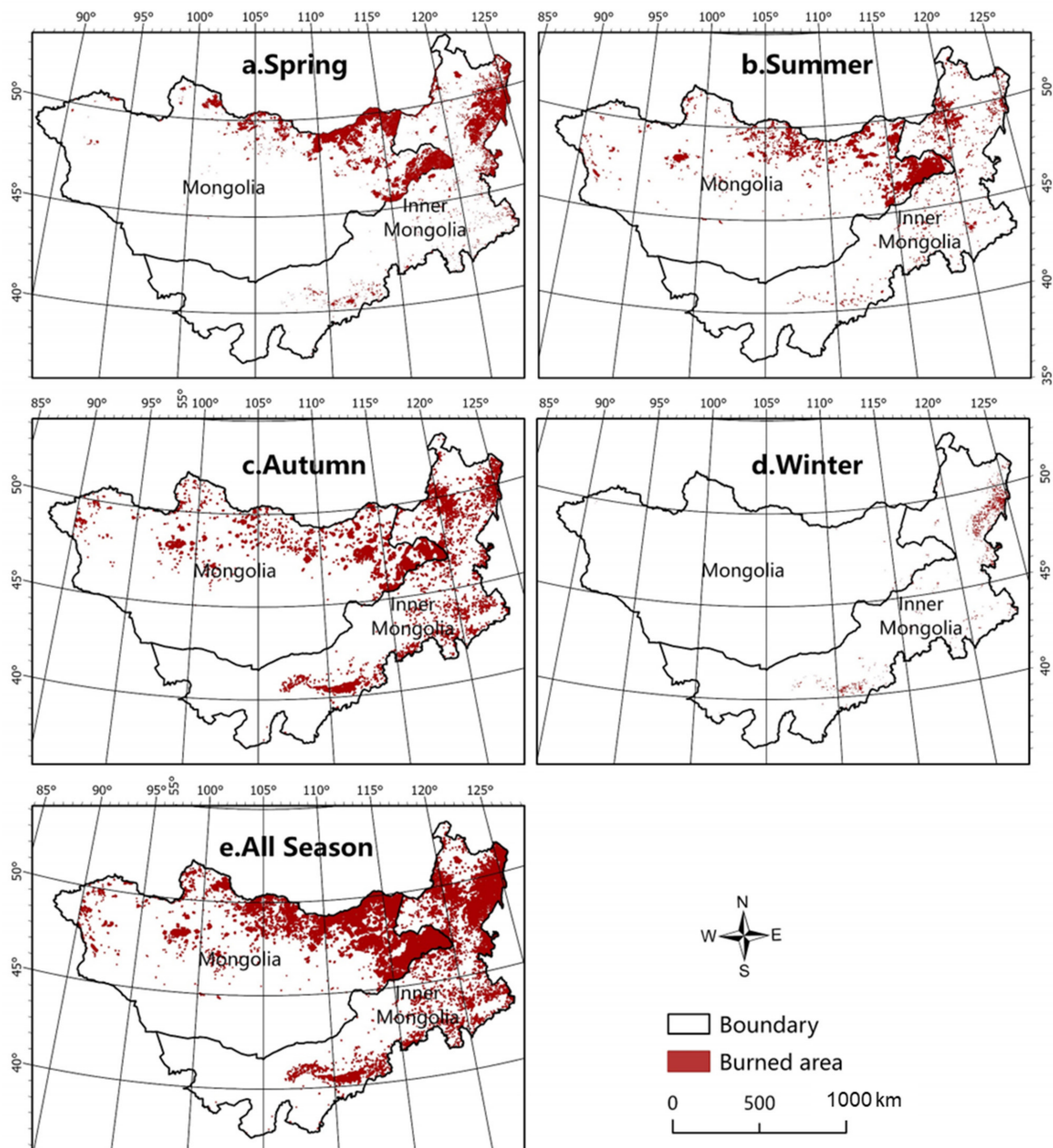

Figure 5. Burned area distribution map in the Mongolian Plateau from 2001 to 2021. Spring (**a**): 57% of the burned area occurred in spring; Summer (**b**): 22% of the burned area occurred in summer; Autumn (**c**): 20% of the burned area occurred in autumn; Winter (**d**): only 1% of the burned area occurred in winter. All-season (**e**): 77% of the total burned area of the whole period occurred in Mongolia and only 23% of burned area in Inner Mongolia.
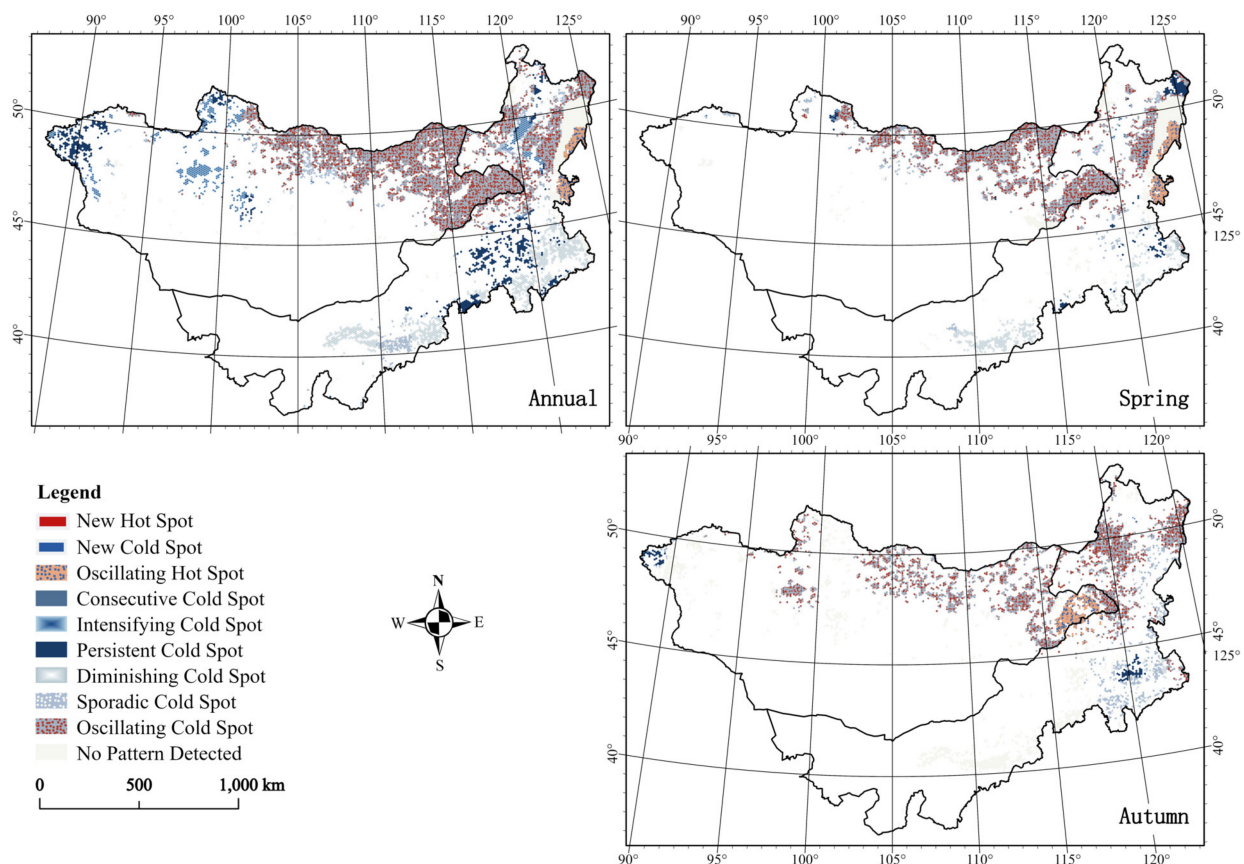
Figure 6. Wildfire pattern changing trend during 2001 to 2021.

4. Discussion

The MP is a region that is extremely sensitive to climate change, such as wildfire and drought, due its traditional grazing practices, highly dependent on its vulnerable highland steppe-dominated ecosystem. Our results identified the distribution patterns and characteristics of fires in both temporal and spatial dimensions. The results demonstrated a roughly decadal fire cycle in the MP (see Figure 3). We predict that the next big fire year (annual burned area over 2.0×10^4 km^2) will be in the year 2024 or 2025. The changing trend of wildfire pattern was also analyzed using a spatiotemporal cube tool in ArcGIS Pro.

Temporally, the environmental factors that determine the occurrence of fires are mainly climate conditions such as temperature, precipitation, and wind. Strong continental monsoons, scarce precipitation, and increasing temperatures effectively reduce the water content of combustible materials and brew the necessary environmental conditions for fires to occur. When spring warmth melts snow off the steppe of eastern Mongolia, the remains the previous year's plant growth is exposed. In dry and windy conditions, brown steppe become tinder for wildfires in spring (Figure 7), which were mainly ignited by human actions such as campfire remnants, the burning of debris, negligently discarded cigarettes, and intentional acts of arson. For these reasons, spring wildfires account for 57% of the total burned area. Wildfire occurrence can also be influenced by surface biomass and vegetation phenology (Figure 7). Fuel load accumulation played an important role in wildfire occurrence, i.e., good vegetation growth and a high fuel load accumulation in the previous year predispose the following spring to wildfire hazards. When a wildfire occurs, fuel load decreases dramatically; therefore, greater wildfires are unlikely to occur in the next year. The area enters a period of relative fire absence while, after a few years of recovery, fuel load will accumulate over time and lead to the next larger wildfire. This explains the peak–valley staggering of over-fire-prone areas between years.
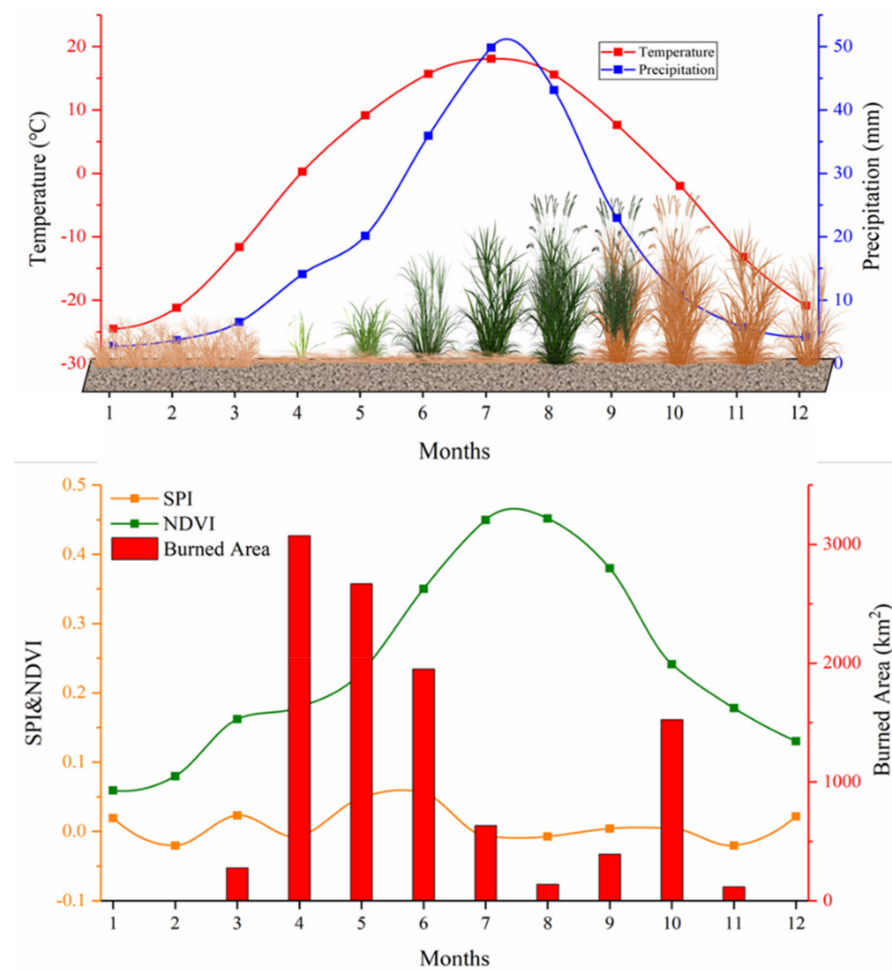
Figure 7. Vegetation phenology drives the intra-annual pattern of wildfire in the Mongolian Plateau (MP).

Spatially, the distribution and spread of fires in the MP are mainly influenced and constrained by human activities. There are three main aspects: First, the management patterns of pasture on both sides of the border between China and Mongolia. Mongolia has always maintained a predominantly nomadic way of life; alternatively, in Inner Mongolia, China, a system of "dual contracting of grass and livestock" and net fencing has been implemented over the last 30 years, transforming herders from nomadic herding to sedentary herding. Chinese herdsmen harvest pastures every autumn to stock up on winter food for their livestock. As a result, on this side of China, there is a low fuel load on the steppe. That is one reason China's side has a lower fire frequency than Mongolia. However, Mongolians practice a nomadic form of herding. The grass is not harvested in the autumn, and, therefore, the Mongolian side has much higher fuel loads on the ground in the following spring, providing large fuel loads for wildfires. A second aspect is the different management patterns of fire on both sides of the border between China and Mongolia. China adopted a strict fire prevention policy, while in Mongolia, wildfires are currently less controlled due to a lack of firefighting teams, and because many of the fires are in remote, high-elevation locations with limited accessibility [41,42]. The principle of wildfire fighting in China is to fight fire in the early stage, in a small situation, and achieve complete extinguishment. Currently, China has the world's largest number of firefighter teams, with 25,000 professional firefighters at the national level and more than 600,000 semi-professional forest firefighters and rescue teams. When a fire is detected on the Mongolian side, Chinese forest firefighters will deploy at the borderline in advance to fight it. As a result, thousands of Chinese firefighters extinguish most of the cross-border fires coming from Mongolia along the borderline (Figure S1c,d). Another reason for the

uncontrolled wildfire on the Mongolia side is the lack of human capacity and technical tools of firefighters. Mongolia is vulnerable to extreme wildfires in spring, and severe droughts frequently occur in summer. A study showed that in 1996 alone, 9 people died and 17 were injured in China in cross-border fires from Mongolia, while 792 livestock died in cross-border fires in China. On the Mongolian side, during the 1996 to 1998 period, 29 people died, 82 were injured, 11,700 heads of livestock perished, and 1066 communication facilities with 263,000 pasture and forest areas burned [43].

In terms of wildfire's changing patterns, the MP fires show a decreasing trend from 2001 to 2021. An oscillating decreasing trend, highly dependent on weather and fuel moisture conditions, was found mainly in the northern forest in Selenge and the steppe in Khentii, Dornod, and Sukhbaatar aimags, especially in the regions near the Mongolia–Russia and Mongolia-China borders. Fires in southern parts of the Great Xing'an Mountain region, under highly strict fuel management, also showed an oscillating decreasing trend, indicating that prescribed burns effectively prevent fires in China. Fuel reduction may be a useful strategy for specific places, but we must be clearly aware that a much more flexible strategy of planning for coexistence with fire is needed for vast parts of the MP. Wildfires in the Xilingol League of Inner Mongolia, China, showed a persistent decreasing trend, due to a lower fuel load, with a much larger number of livestock than that of Mongolia, and due to the positive fire prevention policy in China. Wildfire in the northeastern part of Mongolia also showed a persistent decreasing trend, which may be because of an increase in fuel moisture due to the thawing of the permafrost in recent years in this region [44,45]. It is important to note that fires in the southern region of Dornod aimag in spring, and eastern parts of Great Xing'an Mountain in China in autumn, showed a sporadic increasing trend; these should be the priority regions for future fire prevention for both Mongolia and China. However, herds must live in fire-prone regions in the MP. Fire must be managed on par with other naturally occurring hazards [46]. The underlying causes for a dramatic increase in forest and steppe fires in the MP are deeply rooted in the changing climate and socioeconomic conditions of the country.

Both China and Mongolia's governments have recently taken significant steps in improving wildfire management. For future development of wildfire management, the areas of particular concern are: First, an Early Warning System should be built. Faster fire detection means smaller fires that are controlled more easily. A system of timely and accurate information acquisition, fully integrating the monitoring network and cutting-edge technology in related fields, is an urgent need for both Mongolia and China. Second, better maps of fire hazards, ecosystem functions, and climate change effects to assess trade-offs between development and fire hazard must be developed [46]. Big surprises, such as megadroughts, larger fires, species extirpations, loss of resilience, and system collapses, must be anticipated, and these events must be incorporated into planning. Third, extreme drought events and fire events must be anticipated and incorporated in planning.

5. Conclusions

In this study, we first investigated the temporal distributions of past wildfires in the MP, divided by intra-annual and inter-annual burned areas, and the changes observed in the past two decades. Annual totals derived from satellite data showed good agreement with independent annual estimates available for Mongolia and Inner Mongolia, China. The trend of wildfires in different time scales (yearly, seasonal, and monthly), as well as the distribution of wildfires across different spatial scales (Mongolia, Inner Mongolia, China, and administrative units), were mapped and visualized in the MP from 2001 to 2021. We estimated the annual burned area for 2001–2021 to vary between 0.2×10^4 km^2 and 2.7×10^4 km^2, with the maximum occurring in 2003 and the minimum in 2021. The most extensive burning occurred in the Dornod aimag of Mongolia, accounting for 51% of the total burned area in the MP. The results showed that the wildfires in the MP exhibited a significant temporal dynamic pattern. The peak and trough of the burned area were found to exhibit a significant alternating pattern, with a corresponding decreasing trend also

observed. The extent of area burned by wildfires each year appears to have a fluctuating downward trend. The annual burned area in the latter decade (2012–2021) declined by 38% compared to the previous decade (2001–2010). The study confirmed that the most fire-prone region is only 10% of the land area of the MP; yet, it is home to 90% of all burned areas. Only 1300 km, in the northeastern part of the entire 4710 km border length, are high fire-risk regions. Fires in the MP show a decreasing trend, overall, from 2001 to 2021. The southern region of Dornod aimag and eastern parts of the Great Xing'an Mountain showed a sporadic increasing trend; these should be the priority areas for future fire protection for Mongolia and China. This indicated that the occurrence of steppe wildfire was not a random process; fuel loads, dry weather, and human fire practice may be key drivers for fire occurrence. It is vital that ecologists and fire prevention departments continue to monitor how fire distribution patterns change in the future.

Supplementary Materials: The following are available online at https://www.mdpi.com/article/10.3390/rs15010190/s1, Figure S1: Fire distribution in administrative units in the Mongolian Plateau (MP) and a cross-border fire case, Figure S2: Map of the most fire-prone region near the China-Mongolia border, Figure S3: Statistical summary of wildfire changing trend modes in the Mongolia plateau (MP), Table S1: Definitions of the classification of emerging hot and cold spot analysis in ArcGIS Pro 3.0.

Author Contributions: Conceptualization, Y.B. and K.Y.; methodology, Y.B., M.S. and K.Y.; software, X.F. and N.L.; validation, H.X., Y.Y. and X.F.; formal analysis, K.Y.; investigation, E.N. and B.D.; resources, Y.B. and M.S.; data curation, X.F. and N.L.; writing—original draft preparation, K.Y.; writing—review and editing, K.Y., Y.B., M.S. and E.N.; visualization, Y.B. and K.Y.; supervision, M.S. and L.S.; project administration, Y.B. and K.Y.; funding acquisition, Y.B., K.Y. and B.N.; All authors have read and agreed to the published version of the manuscript. K.Y. and Y.B. contributed equally to this work.

Data Availability Statement: The original burned area data used in this study can be obtained from https://ladsweb.modaps.eosdis.nasa.gov/search/order/2/MCD64A1--6 (accessed on 23 December 2022). The generated data in the study are available from the corresponding author upon reasonable request.

Conflicts of Interest: The authors declare no conflict of interest.

References

1. Pausas, J.G.; Keeley, J.E. Wildfires and global change. *Front. Ecol. Environ.* **2021**, *19*, 387–395. [CrossRef]
2. Bowman, D.; Kolden, C.A.; Abatzoglou, J.T.; Johnston, F.H.; van der Werf, G.R.; Flannigan, M. Vegetation fires in the Anthropocene. *Nat. Rev. Earth Environ.* **2020**, *1*, 500–515. [CrossRef]
3. Xu, R.B.; Yu, P.; Abramson, M.J.; Johnston, F.H.; Samet, J.M.; Bell, M.L.; Haines, A.; Ebi, K.L.; Li, S.S.; Guo, Y.M. Wildfires, Global Climate Change, and Human Health. *N. Engl. J. Med.* **2020**, *383*, 2173–2181. [CrossRef] [PubMed]
4. Melia, N.; Dean, S.; Pearce, H.G.; Harrington, L.; Frame, D.J.; Strand, T. Aotearoa New Zealand's 21st-Century Wildfire Climate. *Earths Future* **2022**, *10*, e2022EF002853. [CrossRef]
5. Ward, M.; Carwardine, J.; Watson, J.E.M.; Pintor, A.; Stuart, S.; Possingham, H.P.; Rhodes, J.R.; Carey, A.R.; Auerbach, N.; Reside, A.; et al. How to prioritize species recovery after a megafire. *Conserv. Biol.* **2022**, *36*, e13936. [CrossRef]
6. Wu, D.Y.; Niu, X.Y.; Chen, Z.Q.; Chen, Y.; Xing, Y.X.; Cao, X.Y.; Liu, J.z.; Wang, X.; Pu, W. Causes and Effects of the Long-Range Dispersion of Carbonaceous Aerosols From the 2019-2020 Australian Wildfires. *Geophys. Res. Lett.* **2022**, *49*, e2022GL099840. [CrossRef]

7. Yuan, S.; Bao, F.; Zhang, X.; Li, Y. Severe Biomass-Burning Aerosol Pollution during the 2019 Amazon Wildfire and Its Direct Radiative-Forcing Impact: A Space Perspective from MODIS Retrievals. *Remote Sens.* **2022**, *14*, 2080. [CrossRef]
8. Buotte, P.C.; Levis, S.; Law, B.E.; Hudiburg, T.W.; Rupp, D.E.; Kent, J.J. Near-future forest vulnerability to drought and fire varies across the western United States. *Glob. Chang. Biol.* **2019**, *25*, 290–303. [CrossRef]
9. Burke, M.; Driscoll, A.; Heft-Neal, S.; Xue, J.; Burney, J.; Wara, M. The changing risk and burden of wildfire in the United States. *Proc. Natl. Acad. Sci. USA* **2021**, *118*, e2011048118. [CrossRef]
10. Hyde, A.S.; Verstraeten, B.S.E.; Olson, J.K.; King, S.; Bremault-Phillips, S.; Olson, D.M. The Fort McMurray Mommy Baby Study: A Protocol to Reduce Maternal Stress Due to the 2016 Fort McMurray Wood Buffalo, Alberta, Canada Wildfire. *Front. Public Health* **2021**, *9*, 685. [CrossRef]
11. Skakun, R.; Castilla, G.; Metsaranta, J.; Whitman, E.; Rodrigue, S.; Little, J.; Groenewegen, K.; Coyle, M. Extending the National Burned Area Composite Time Series of Wildfires in Canada. *Remote Sens.* **2022**, *14*, 3050. [CrossRef]
12. Allan, R.P.; Arias, P.A.; Berger, S.; Canadell, J.G.; Cassou, C.; Chen, D.; Cherchi, A.; Connors, S.L.; Coppola, E.; Cruz, F.A.; et al. *Climate Change 2021: The Physical Science Basis*; Cambridge University: Cambridge, UK, 2021.
13. Zhongming, Z.; Linong, L.; Xiaona, Y.; Wangqiang, Z.; Wei, L. Climate Risk Country Profile: Mongolia. 2021. Available online: https://www.adb.org/publications/climate-risk-country-profile-mongolia (accessed on 30 June 2021).
14. Neupert, R.F. Population, nomadic pastoralism and the environment in the Mongolian Plateau. *Popul. Environ.* **1999**, *20*, 413–441. [CrossRef]
15. Rao, M.P.; Davi, N.K.; D D'Arrigo, R.; Skees, J.; Nachin, B.; Leland, C.; Lyon, B.; Wang, S.-Y.; Byambasuren, O. Dzuds, droughts, and livestock mortality in Mongolia. *Environ. Res. Lett.* **2015**, *10*, 74012. [CrossRef]
16. Zhang, P.; Jeong, J.H.; Yoon, J.H.; Kim, H.; Wang, S.Y.S.; Linderholm, H.W.; Fang, K.Y.; Wu, X.C.; Chen, D.L. Abrupt shift to hotter and drier climate over inner East Asia beyond the tipping point. *Science* **2020**, *370*, 1095–1099. [CrossRef]
17. Bai, Y.; Li, S.; Liu, M.; Guo, Q. Assessment of vegetation change on the Mongolian Plateau over three decades using different remote sensing products. *J. Environ. Manag.* **2022**, *317*, 115509. [CrossRef]
18. Nanzad, L.; Zhang, J.H.; Tuvdendorj, B.; Nabil, M.; Zhang, S.; Bai, Y. NDVI anomaly for drought monitoring and its correlation with climate factors over Mongolia from 2000 to 2016. *J. Arid. Environ.* **2019**, *164*, 69–77. [CrossRef]
19. Tao, S.L.; Fang, J.Y.; Zhao, X.; Zhao, S.Q.; Shen, H.H.; Hu, H.F.; Tang, Z.Y.; Wang, Z.H.; Guo, Q.H. Rapid loss of lakes on the Mongolian Plateau. *Proc. Natl. Acad. Sci. USA* **2015**, *112*, 2281–2286. [CrossRef]
20. Kimura, R.; Moriyama, M. Use of A MODIS Satellite-Based Aridity Index to Monitor Drought Conditions in Mongolia from 2001 to 2013. *Remote Sens.* **2021**, *13*, 2561. [CrossRef]
21. Saladyga, T.; Hessl, A.; Nachin, B.; Pederson, N. Privatization, Drought, and Fire Exclusion in the Tuul River Watershed, Mongolia. *Ecosystems* **2013**, *16*, 1139–1151. [CrossRef]
22. Bao, G.; Bao, Y.L.; Bao, Y.H.; Amarjargal; Hang, Y.L. Spatiotemporal Variations in Fire Behavior in the Mongolian Plateau during 2001-2012. *Adv. Intel. Sys. Res.* **2014**, *102*, 507–511.
23. John, R.; Chen, J.; Ou-Yang, Z.-T.; Xiao, J.; Becker, R.; Samanta, A.; Ganguly, S.; Yuan, W.; Batkhishig, O. Vegetation response to extreme climate events on the Mongolian Plateau from 2000 to 2010. *Environ. Res. Lett.* **2013**, *8*, 35033. [CrossRef]
24. Zhao, H.; Zhang, Z.X.; Ying, H.; Chen, J.H.; Zhen, S.; Wang, X.; Shan, Y.L. The spatial patterns of climate-fire relationships on the Mongolian Plateau. *Agric. For. Meteorol.* **2021**, *308*, 108549. [CrossRef]
25. Danilin, I.M.; Tsogt, Z. Dynamics of structure and biological productivity of post-fire larch forests in the Northern Mongolia. *Contemp. Probl. Ecol.* **2014**, *7*, 158–169. [CrossRef]
26. Nasanbat, E.; Lkhamjav, O.; Balkhai, A.; Tsevee-Oirov, C.; Purev, A.; Dorjsuren, M. A spatial distributionmap of the wildfire risk in Mongolia using decision support system. *Int. Arch. Photogramm. Remote Sens. Spat. Inf. Sci.* **2018**, *42*, 357–362. [CrossRef]
27. Kazato, M.; Soyollham, B. Forest-steppe fires as moving disasters in the Mongolia-Russian borderland. *J. Contemp. East Asia Stud.* **2022**, *11*, 22–45. [CrossRef]
28. van der Werf, G.R.; Randerson, J.T.; Giglio, L.; Collatz, G.J.; Mu, M.; Kasibhatla, P.S.; Morton, D.C.; DeFries, R.S.; Jin, Y.; van Leeuwen, T.T. Global fire emissions and the contribution of deforestation, savanna, forest, agricultural, and peat fires (1997–2009). *Atmos. Chem. Phys.* **2010**, *10*, 11707–11735. [CrossRef]
29. Giglio, L.; Csiszar, I.; Justice, C.O. Global distribution and seasonality of active fires as observed with the Terra and Aqua Moderate Resolution Imaging Spectroradiometer (MODIS) sensors. *J. Geophys. Res. Biogeosci.* **2006**, *111*. [CrossRef]
30. Loboda, T.V.; Hoy, E.E.; Giglio, L.; Kasischke, E.S. Mapping burned area in Alaska using MODIS data: A data limitations-driven modification to the regional burned area algorithm. *Int. J. Wildland Fire* **2011**, *20*, 487–496. [CrossRef]
31. Giglio, L.; Boschetti, L.; Roy, D.P.; Humber, M.L.; Justice, C.O. The Collection 6 MODIS burned area mapping algorithm and product. *Remote Sens. Environ.* **2018**, *217*, 72–85. [CrossRef]
32. Giglio, L.; Randerson, J.T.; van der Werf, G.R. Analysis of daily, monthly, and annual burned area using the fourth-generation global fire emissions database (GFED4). *J. Geophys. Res. Biogeosci.* **2013**, *118*, 317–328. [CrossRef]
33. Artes, T.S.; Oom, D.; De Rigo, D.; Durrant, T.H.; Maianti, P.; Liberta, G.; San-Miguel-Ayanz, J. A global wildfire dataset for the analysis of fire regimes and fire behaviour. *Sci. Data* **2019**, *6*, 296. [CrossRef]
34. Boschetti, L.; Roy, D.P.; Giglio, L.; Huang, H.; Zubkova, M.; Humber, M.L. Global validation of the collection 6 MODIS burned area product. *Remote Sens. Environ.* **2019**, *235*, 111490. [CrossRef]

35. Rodrigues, J.A.; Libonati, R.; Pereira, A.A.; Nogueira, J.M.P.; Santos, F.L.M.; Peres, L.F.; Santa Rosa, A.; Schroeder, W.; Pereira, J.M.C.; Giglio, L.; et al. How well do global burned area products represent fire patterns in the Brazilian Savannas biome? An accuracy assessment of the MCD64 collections. *Int. J. Appl. Earth Obs.* **2019**, *78*, 318–331. [CrossRef]

36. Giglio, L.; Schroeder, W.; Justice, C.O. The collection 6 MODIS active fire detection algorithm and fire products. *Remote Sens. Environ.* **2016**, *178*, 31–41. [CrossRef]

37. Rihan, W.; Zhao, J.; Zhang, H.; Guo, X.; Ying, H.; Deng, G.; Li, H. Wildfires on the Mongolian Plateau: Identifying drivers and spatial distributions to predict wildfire probability. *Remote Sens.* **2019**, *11*, 2361. [CrossRef]

38. Wenfeng, C.; Hongyan, Z.; Kunpeng, X.; Yuhai, B. Spatiotemporal patterns and trends of the Mongolian Plateau wildfires. Природа Внутренней Азии **2017**, *4*, 13–25.

39. Esri. Sentinel-2 10 m Land Use/Land Cover Time Series. Available online: https://www.arcgis.com/home/item.html?id=d3da5 dd386d140cf93fc9ecbf8da5e31 (accessed on 10 February 2022).

40. Na, L.; Zhang, J.Q.; Bao, Y.L.; Bao, Y.B.; Na, R.S.; Tong, S.Q.; Si, A.; Na, L.; Zhang, J.; Bao, Y.; et al. Himawari-8 Satellite Based Dynamic Monitoring of Grassland Fire in China-Mongolia Border Regions. *Sensors* **2018**, *18*, 276. [CrossRef]

41. Dionne, R.; Shulman, D. *Mongolia Wildfire Assessment*; United States Forest Service: Washington, DC, USA, 1996; pp. 1–13.

42. Darren, J.; Byambasuren, O.; Babler, M. *Fire Management Assessment of the Eastern Steppe, Mongolia*; The Nature Conservancy: Arlington, VA, USA, 2009; pp. 1–42.

43. Farukh, M.A.; Hayasaka, H.; Mishigdorj, O. Recent tendency of Mongolian wildland fire incidence: Analysis using MODIS hotspot and weather data. *J. Nat. Disaster Sci.* **2009**, *31*, 23–33. [CrossRef]

44. Dashtseren, A.; Temuujin, K.; Westermann, S.; Batbold, A.; Amarbayasgalan, Y.; Battogtokh, D. Spatial and Temporal Variations of Freezing and Thawing Indices From 1960 to 2020 in Mongolia. *Front. Earth Sci.* **2021**, *9*, 713498. [CrossRef]

45. Munkhjargal, M.; Yadamsuren, G.; Yamkhin, J.; Menzel, L. The Combination of Wildfire and Changing Climate Triggers Permafrost Degradation in the Khentii Mountains, Northern Mongolia. *Atmosphere-Basel* **2020**, *11*, 155. [CrossRef]

46. Moritz, M.A.; Batllori, E.; Bradstock, R.A.; Gill, A.M.; Handmer, J.; Hessburg, P.F.; Leonard, J.; McCaffrey, S.; Odion, D.C.; Schoennagel, T.; et al. Learning to coexist with wildfire. *Nature* **2014**, *515*, 58–66. [CrossRef] [PubMed]